Metabolic Control Analysis of glycolysis in tuber tissue of potato (*Solanum tuberosum*): explanation for the low control coefficient of phosphofructokinase over respiratory flux

Simon THOMAS*, Peter J. F. MOONEY†, Michael M. BURRELL† and David A. FELL*‡

*School of Biological and Molecular Sciences, Oxford Brookes University, Oxford OX3 0BP, U.K. and †Advanced Technologies (Cambridge) Ltd., 210 Cambridge Science Park, Cambridge CB4 4WA, U.K.

We have applied Metabolic Control Analysis (MCA) in an attempt to determine the distribution of glycolytic flux control between the steps of glycolysis in aged disks of potato tuber under aerobic conditions, using concentrations of glycolytic metabolites in tuber tissue from a range of transgenic potato plants and published enzyme kinetic data. We modelled the substrate and effector kinetics of potato tuber phosphofructokinase (PFK) by reanalysing published results. Despite the scarcity of reliable kinetic data, our results are in agreement with experimental findings namely that, under the conditions described, PFK has little control over glycolytic flux. Furthermore our analysis predicts that under these conditions far more control lies in the dephosphorylation of phosphoenolpyruvate and/or in the steps beyond. We have validated the results of our analysis in two ways. First, predictions based on calculated concentration control coefficients from the analysis show generally good agreement with observed metabolite deviation indices discussed in the preceding paper [Thomas, Mooney, Burrell, and Fell (1997) *Biochem. J.* **322**, 111–117]. Second, sensitivity analysis of our results shows that the calculated control coefficients are robust to errors in the elasticities used in the analysis, of which relatively few need to be known accurately. Experimental and control analysis results agree with previous predictions of MCA that strong co-operative feedback inhibition of enzymes serves to move flux control downstream of the inhibiting metabolite. We conclude that MCA can successfully model the outcome of experiments in the genetic manipulation of enzyme amounts.

INTRODUCTION

In the preceding paper [1] we described how the finite change method of Metabolic Control Analysis (MCA) [2] could be applied to interpret the metabolite changes occurring in aged disks from tubers of transgenic potato plants expressing different amounts of *Escherichia coli* phosphofructokinase (PFK) A. Despite massive overexpression of PFK, this transgenic tissue showed no significant changes in the fluxes through either respiration or glycolysis [3,4]. We showed that the effects on glycolytic metabolite concentrations were consistent with those expected from successful amplification of PFK activity *in vivo*, but the changes showed that between fructose 1,6-bisphosphate (F16BP) and pyruvate the signal of increased PFK activity (namely increased F16BP concentration) was attenuated, resulting in the observed lack of flux change.

In this paper, we describe how a complementary approach using MCA [5,6] produced results in agreement with these findings. From a consideration of metabolite levels in the control plants only, and literature values of the kinetic parameters of the glycolytic enzymes, we show that PFK is predicted to have a low flux control coefficient over both glycolysis and respiration in aged disks of potato tuber. Furthermore our analysis predicts that far more flux control over respiration lies in the oxidative metabolism of phosphoenolpyruvate (PEP) than in the glycolytic segment of the pathway. The low flux control coefficient of PFK is explained by MCA [5,6] as a consequence of its strong feedback inhibition by PEP.

We discuss the benefits and limitations of using MCA in this way to predict the distribution of pathway control, as well as the prospects of understanding the behaviour of complex metabolic pathways with a view to successfully directing genetic manipulation of organisms.

MATERIALS AND METHODS

Details of production of the transgenic plants along with assays for metabolites and PFK are in [4]. Non-linear fitting of PFK kinetics was performed using the program Statistica for Windows (Statsoft Inc., Tulsa, U.S.A.) running on an IBM-compatible PC.

Abbreviations used: 13BPG, 1,3-bisphosphoglycerate; 2PGA, 2-phosphoglycerate; 3PGA, 3-phosphoglycerate; aldolase, fructosebisphosphate aldolase (D-fructose-1,6-bisphosphate-D-glyceraldehyde-3-phosphate-lyase, EC 4.1.2.13); DHAP, dihydroxyacetone phosphate; enolase, phosphopyruvate hydratase (2-phospho-D-glycerate hydrolyase, EC 4.2.1.11); F16BP, fructose 1,6-bisphosphate; F6P, fructose 6-phosphate; G1P, glucose 1-phosphate; G6P, glucose 6-phosphate; GAP, glyceraldehyde 3-phosphate; GAPDH, glyceraldehyde-3-phosphate dehydrogenase [D-glyceraldehyde-3-phosphate–NAD^+ oxidoreductase (phosphorylating), EC 1.2.1.12]; GUS, β-glucuronidase (β-D-glucuronide glucuronosohydrolase, EC 3.2.1.31); PEP, phosphoenolpyruvate; PFK, 6-phosphofructokinase (ATP–D-fructose-6-phosphate 1-phosphotransferase, EC 2.7.1.11); PFP, pyrophosphate-dependent 6-phosphofructokinase (pyrophosphate–D-fructose-6-phosphate 1-phosphotransferase, EC 2.7.1.90); PGI, phosphoglucose isomerase (D-glucose-6-phosphate ketol-isomerase, EC 5.3.1.9); PGK, phosphoglycerate kinase (ATP–3-phospho-D-glycerate 1-phosphotransferase, EC 2.7.2.3); PGM, phosphoglucomutase (α-D-glucose-1-phosphate phosphotransferase, EC 5.4.2.2); PGlyM, phosphoglycerate mutase (2-phospho-D-glycerate phosphotransferase, EC 5.4.2.1); PK, pyruvate kinase (ATP–pyruvate 2-*O*-phosphotransferase, EC 2.7.1.40); TPI, triosephosphate isomerase (D-glyceraldehyde-3-phosphate ketol-isomerase, EC 5.3.1.1); MCA, Metabolic Control Analysis.

‡ To whom correspondence should be addressed.

Metabolic Control Analysis

Measured amounts of metabolites (mmol/kg wet weight) from [4] were converted into approximate cytosolic concentrations (mM) by multiplying by 10, assuming that the cytosolic volume is approximately 10% of the cell volume, and ignoring possible partitioning between the cytosol and amyloplasts. Along with published enzyme kinetic data, these concentrations were used to estimate elasticities for each of the effector/enzyme interactions in the control and transgenic plants *in vivo*. From the elasticities we simultaneously calculated the flux and concentration control coefficients of all of the steps of glycolysis, using the matrix method of Fell and Sauro [7]. The approach is similar to that used in the study of rat hepatocyte gluconeogenesis [8], liver serine biosynthesis [9] and rat heart glycolysis [10]. Definitions and symbols for MCA terms are described in [6,11].

Elasticities were obtained by differentiating and scaling the enzyme rate laws (kinetic parameters used are in Appendices 1 and 2), except for phosphoglucomutase (PGM), glyceraldehyde-3-phosphate dehydrogenase (GAPDH) and phosphoglycerate kinase (PGK). Because 1,3-bisphosphoglycerate (1,3BPG) could not be measured accurately, and there were no values for NAD^+ or NADH, GAPDH and PGM were combined into a single step and arbitrarily assigned an overall disequilibrium ratio of 0.4 for all four lines. PGM and the combined GAPDH/PGK steps were treated using the near-equilibrium approximation [8].

Glucose 1-phosphate (G1P) and pyruvate were designated as pool metabolites, marking the beginning and end of the pathway segment under consideration, as were ATP, ADP, P_i and PP_i. As with any model, its behaviour can only approximate that of the real system, and care must be taken both in choosing the actual model structure and in interpreting the results. This is especially true of a central pathway such as glycolysis. Not only is it linked to every area of metabolism through its cofactors, but its pathway intermediates are linked to other pathways of carbon metabolism, most crucially the pentose phosphate pathway. G1P was chosen as the source metabolite since the concentration of this immediate product of starch breakdown is maintained at near-constant levels. There were virtually no significant differences in its concentrations between any of the lines considered here [4]. Pyruvate was regarded as the end of the pathway since, although its concentration did change [4], pyruvate kinase (PK) was the only enzyme affected, and that only weakly. ATP, ADP, P_i and PP_i were defined as pools because there is no reliable quantitative kinetic information on how their concentrations are affected by other areas of metabolism. ATP, ADP and PP_i were measured for each set of conditions studied [4]. P_i concentration was calculated assuming that the reaction catalysed by pyrophosphate-dependent phosphofructokinase (PFP) was at equilibrium, with $K_{eq} = 3.3$ in the glycolytic direction [12].

Calculation of the elasticities and the control coefficients was automated using the computer program MetaCon [13]. The input required for MetaCon was: (i) a reaction scheme for the pathway; (ii) algebraic expressions for the elasticities in terms of enzyme kinetic parameters and metabolite concentrations (Appendices 1 and 2); (iii) values for the kinetic parameters (Appendices 1 and 2) and the metabolite concentrations [14]. Sensitivity analysis of the control coefficients, which requires no extra data, was also carried out by MetaCon.

RESULTS AND DISCUSSION

Elasticity coefficients

Before considering the actual distribution of flux and concentration control coefficients, it is necessary to check the elasticities (Table 1) for any obvious anomalies resulting from the choice of model parameters, so as to be aware of how they might influence the calculated control coefficients. Studying the elasticities for the GUS control plants (column 1 of Table 1) the most obvious anomaly is that the substrate elasticities $\epsilon^{\mathrm{aldolase}}_{\mathrm{F16BP}}$, $\epsilon^{\mathrm{TPI}}_{\mathrm{DHAP}}$ and $\epsilon^{\mathrm{PGlyM}}_{\mathrm{3PGA}}$ are negative, whereas the product elasticities $\epsilon^{\mathrm{aldolase}}_{\mathrm{DHAP}}$, $\epsilon^{\mathrm{aldolase}}_{\mathrm{GAP}}$, $\epsilon^{\mathrm{TPI}}_{\mathrm{GAP}}$ and $\epsilon^{\mathrm{PGlyM}}_{\mathrm{2PGA}}$ are positive. All these negated elasticities arise as a result of the calculated disequilibrium ratios for aldolase, TPI and PGlyM being greater than 1. In the transgenic lines PFK-36 and PFK-22, $\epsilon^{\mathrm{PGlyM}}_{\mathrm{3PGA}}$ and $\epsilon^{\mathrm{PGlyM}}_{\mathrm{2PGA}}$ have the correct signs. The negated elasticities imply that the flux through the steps displaying them is in the reverse, or gluconeogenic, direction. This is not a conceivable explanation for PGlyM. It is also highly unlikely for TPI and aldolase, as it would require a large recycling oxidative pentose phosphate pathway flux and a correspondingly large net flux from F16BP to F6P via PFP. Thus, although this is a possible explanation for TPI and aldolase, more probable explanations are that the measured metabolite concentrations do not accurately reflect the free concentrations in the cytosol, and/or the equilibrium constants used are not correct for the cytosolic conditions in potato tuber (this second explanation being a particularly likely candidate). One thing that is certain, however, is that the metabolism around F16BP and the triose phosphates, especially in tissues with an active oxidative pentose phosphate pathway and either PFP or active fructose 1,6-bisphosphatase is likely to be complex. This is illustrated in the preceding paper [1], where the changes in deviation indices with increasing PFK activity indicate that GAP and DHAP do not always appear to be in equilibrium. The effect of the negated elasticities on the concentration and flux control coefficients is discussed in following sections.

The other factor that can immediately be assessed is the use of the near-equilibrium approximation for the elasticities of PGM

Table 1 Elasticities for glycolytic enzymes of GUS control and PFK transgenic plants

Elasticities were calculated from glycolytic metabolite concentrations in aged disks of potato tuber from [4], and enzyme kinetic parameters taken from the literature. $\epsilon^{\mathrm{PFK}}_{\mathrm{F16BP}} = -0.005$ was calculated by comparison between the observed and calculated values of D^{S}_{PFK}. G6P, glucose 6-phosphate; PGI, phosphoglucose isomerase; F6P, fructose 6-phosphate; DHAP, dihydroxyacetone phosphate; GAP, glyceraldehyde 3-phosphate; TPI, triosephosphate isomerase; 3PGA, 3-phosphoglycerate; PGlyM, phosphoglycerate mutase; 2PGA, 2-phosphoglycerate.

	GUS-6	PFK-5	PFK-36	PFK-22
$\epsilon^{\mathrm{PGM}}_{\mathrm{G6P}}$	−10.6	−1.77	−3.45	−1.63
$\epsilon^{\mathrm{PGI}}_{\mathrm{G6P}}$	2.19	2.37	2.34	2.96
$\epsilon^{\mathrm{PGI}}_{\mathrm{F6P}}$	−2.22	−1.69	−1.75	−0.993
$\epsilon^{\mathrm{PFK}}_{\mathrm{F6P}}$	2.35	3.34	3.51	8.25
$\epsilon^{\mathrm{PFK}}_{\mathrm{F16BP}}$	−0.005	−0.005	−0.005	−0.005
$\epsilon^{\mathrm{PFK}}_{\mathrm{PEP}}$	−1.17	−1.82	−1.88	−3.85
$\epsilon^{\mathrm{aldolase}}_{\mathrm{F16BP}}$	−3.90	−3.96	−1.44	−1.30
$\epsilon^{\mathrm{aldolase}}_{\mathrm{DHAP}}$	3.91	3.96	1.44	1.30
$\epsilon^{\mathrm{aldolase}}_{\mathrm{GAP}}$	3.91	3.96	1.44	1.30
$\epsilon^{\mathrm{TPI}}_{\mathrm{DHAP}}$	−0.430	−0.779	−0.558	−0.604
$\epsilon^{\mathrm{TPI}}_{\mathrm{GAP}}$	0.941	1.14	0.766	0.757
$\epsilon^{\mathrm{GAPDH/PGK}}_{\mathrm{GAP}}$	2.69	2.69	2.69	2.69
$\epsilon^{\mathrm{GAPDH/PGK}}_{\mathrm{3PGA}}$	−1.69	−1.69	−1.69	−1.69
$\epsilon^{\mathrm{PGlyM}}_{\mathrm{3PGA}}$	−0.231	−0.691	2.76	0.663
$\epsilon^{\mathrm{PGlyM}}_{\mathrm{2PGA}}$	0.358	0.841	−2.64	−0.579
$\epsilon^{\mathrm{enolase}}_{\mathrm{2PGA}}$	0.404	0.786	1.12	1.71
$\epsilon^{\mathrm{enolase}}_{\mathrm{PEP}}$	−0.150	−0.559	−0.897	−1.51
$\epsilon^{\mathrm{PK}}_{\mathrm{PEP}}$	0.221	0.0584	0.0542	0.102

and GAPDH/PGK. This approximation [8] involves ignoring the effect of the kinetic term in the substrate and product elasticities, just retaining the thermodynamic term of each. Because the kinetic term of an elasticity for a reversible Michaelis–Menten step is always less than 1, it is a good approximation when the moduli of the substrate and product thermodynamic terms are much greater than 1. For ϵ_{G6P}^{PGM} (the elasticity to G1P is not needed, because it is a pool metabolite), this can be seen to be a good approximation for line GUS-6, reasonable for line PFK-36, but possibly poor for lines PFK-5 and PFK-22. The kinetic term is subtracted from the thermodynamic term, so the real values are more negative than those in Table 1, the actual difference depending on the size of the unknown kinetic term. The main result is that the calculated flux control coefficients of PGM in lines PFK-5 and PFK-22 are likely to overestimate slightly the actual values. However, because of the relatively large values of the thermodynamic term of ϵ_{G6P}^{PGM}, even in PFK-5 and PFK-22 the effects are likely to be small [14,15]. Assigning an arbitrary unchanging disequilibrium ratio of 0.4 to GAPDH/PGK artificially forces this combined step to have a low flux control coefficient in all lines, although sensitivity analysis of the model (described below) indicates that the GAPDH/PGK elasticities have virtually no effect on the results.

Determination of ϵ_{F16BP}^{PFK}: relationship between control coefficients and metabolite deviation indices

ϵ_{F16BP}^{PFK} was the only elasticity that could not be assigned an approximate value from the information that was available at the start of this study (see Appendices 1 and 2), as our source of kinetic data for PFK [16] did not include F16BP inhibition kinetics. As the reaction is essentially irreversible, it was immediately apparent that the elasticity would be small, but other than this there was no indication of how its value could be assigned. Varying it over the range $-0.2 < \epsilon_{F16BP}^{PFK} < -0.0001$ caused virtually no change in C_{PFK}^{J}, but there were large changes in the flux and concentration control coefficients of aldolase, TPI, GAPDH/PGK, PGM and enolase. Therefore estimation of the correct value was important in attempting to quantify the response of the metabolite concentrations, but bounds could not be set by observing the value of C_{PFK}^{J}. In order to solve the problem of assigning a value to ϵ_{F16BP}^{PFK} we used the relationship between the flux and concentration control coefficients of 'traditional' MCA and the deviation indices of finite change theory [2,17]:

$$D_{PFK}^{S} = C_{PFK_C}^{S^C} \frac{1}{1-(C_{PFK_C}^{J^C} - C_{PFK_C}^{S^C})\left(\frac{r-1}{r}\right)} \quad (1)$$

where D_{PFK}^{S} is the deviation index for metabolite S for an r-fold increase in PFK activity, $C_{PFK}^{S^C}$ is the concentration control coefficient of PFK for metabolite S evaluated for the control plants, and $C_{PFK}^{J^C}$ the flux control coefficient of PFK for the pathway flux, also evaluated for the control plants. Deviation indices had been calculated for the 8.11-fold increase in PFK activity between the GUS control and PFK-5 lines [1]. These values, together with values calculated from eqn. (1) for the variable metabolites in the model for various values of ϵ_{F16BP}^{PFK} are shown in Table 2. The calculated deviation indices are negative for metabolites upstream of PFK (i.e. G6P and F6P) because activation of PFK will tend to lower their concentrations, and positive for those downstream (i.e. F16BP to PEP) for the opposite reason. As can be seen by comparing column 1 with columns 2–7 in Table 2, agreement between the measured and calculated deviation indices is good, in most cases the two values for each index being within a factor of 2 or 3 of one another, and with an excellent agreement for GAP. The exceptions are G6P, F6P and 2PGA. There is no possibility of an agreement between the indices for 2PGA because of the unexpected decrease observed in 2PGA concentration. Consequently the observed deviation index is negative. This observation is discussed at greater length in [1]. The apparently poor agreement for G6P and, especially, for F6P is particularly surprising as this latter metabolite is the immediate substrate of PFK. It could suggest that factors outside our model influence the concentrations, the most likely candidate being PFP or, possibly, the reactions of the oxidative pentose phosphate pathway (which can also be expected to influence the values for F16BP and GAP respectively). However, the experimental values for these deviation indices had particularly large errors [1], so it is not significant that these discrepancies are not significant.

Table 2 Correspondence between measured and calculated deviation indices

Column 1 contains observed deviation indices for the transformation from the GUS 6 control line to PFK-5 as calculated in [1]. Columns 2 to 7 contain deviation indices calculated for different values of ϵ_{F16BP}^{PFK} using $D_{PFK}^{S} = C_{PFK_C}^{S^C} 1/\{1-(C_{PFK_C}^{J^C} - C_{PFK_C}^{S^C})[(r-1)/r]\}$, where D_{PFK}^{S} is the deviation index for metabolite S for an r-fold increase in PFK activity, $C_{PFK}^{S^C}$ is the concentration control coefficient of PFK for metabolite S evaluated for the control plant, and $C_{PFK}^{J^C}$ the flux control coefficient of PFK for the pathway flux, also evaluated for the control plants. Each value of ϵ_{F16BP}^{PFK} generates different values of $C_{PFK}^{S^C}$ and $C_{PFK}^{J^C}$. Flux and concentration control coefficients were calculated using the computer program MetaCon. The value $\epsilon_{F16BP}^{PFK} = -0.005$ used in the MCA calculations was chosen as the approximate value where the observed and calculated values of D_{PFK}^{S} first show the closest convergence (column 5).

		D_{PFK}^{S} calculated for ϵ_{F16BP}^{PFK} equal to:					
Metabolite	Observed D_{PFK}^{S}	−1	−0.1	−0.01	−0.005	−0.001	−0.0001
G6P	−0.33	−0.01	−0.01	−0.01	−0.01	−0.01	−0.01
F6P	−0.50	−0.06	−0.08	−0.09	−0.09	−0.09	−0.09
F16BP	0.75	0.24	0.30	0.31	0.31	0.31	0.31
DHAP	0.65	0.13	0.17	0.17	0.18	0.18	0.18
GAP	0.21	0.15	0.20	0.21	0.21	0.21	0.21
3PGA	0.53	0.19	0.24	0.25	0.25	0.25	0.25
2PGA	−0.48	0.32	0.39	0.40	0.40	0.40	0.40
PEP	0.82	0.34	0.41	0.42	0.42	0.42	0.42

The generally good agreement shown between the observed and predicted values of the deviation indices for the metabolites is particularly good evidence for the accuracy of the model. Given the assumptions made, the agreement is better than could reasonably be expected. The absolute magnitudes of calculated concentration control coefficients are highly sensitive to inaccuracies in the equations used to calculate them, much more so than are flux control coefficients. In this context, 'inaccuracies' include: aldolase, TPI and PGlyM concentration control coefficients with incorrect sign because of the negated elasticity values; the omission from consideration of PFP and the reaction of the oxidative pentose phosphate pathway; the omission from consideration of many possible regulatory phenomena, other than feedback inhibition of PEP on PFK; the use of kinetic parameters from tissue other than potato tuber.

The excellent agreement between calculated and observed values for GAP is somewhat paradoxical, because it is one of the metabolites that shows low constancy of its deviation index with different r-fold changes in PFK activity [1], which would imply that the linear approximation implicit in the application of eqn. (1) is not valid in the case of GAP. Also, GAP concentration is likely to be affected by the pentose phosphate pathway flux, a

Table 3 Calculated concentration control coefficients for glycolytic enzymes of GUS control plants

C^S_E is the concentration control coefficient of enzyme E over metabolite S, where each metabolite corresponds to a particular column. Concentration control coefficients were calculated using the computer program MetaCon.

	G6P	F6P	F16BP	DHAP	GAP	3PGA	2PGA	PEP
C^S_{PGM}	0.09	0.08	0.08	0.04	0.05	0.06	0.12	0.13
C^S_{PGI}	−0.01	0.37	0.39	0.19	0.24	0.29	0.58	0.63
C^S_{PFK}	−0.01	−0.07	0.37	0.18	0.22	0.28	0.55	0.60
$C^S_{aldolase}$	0.00	0.00	0.26	−0.00	−0.00	−0.00	−0.00	−0.00
C^S_{TPI}	0.00	0.00	2.32	2.32	−0.00	−0.00	−0.01	−0.01
$C^S_{GAPDH/PGK}$	−0.00	−0.00	−1.18	−0.81	−0.37	0.00	0.00	0.00
C^S_{PGlyM}	−0.00	−0.00	8.68	5.96	2.72	4.32	−0.02	−0.03
$C^S_{enolase}$	−0.00	−0.00	−7.69	−5.28	−2.41	−3.83	−2.46	0.02
C^S_{PK}	−0.07	−0.38	−3.24	−2.61	−0.44	−1.12	1.24	−1.35

factor not incorporated into our model. Conversely, DHAP and PEP, which do show good constancy of their deviation indices, show poorer agreement between observed and calculated values.

Table 2 shows that, in all cases except 2PGA, the observed deviation indices are closest to the calculated with small, rather than large, values of $|\epsilon^{PFK}_{F16BP}|$. As $|\epsilon^{PFK}_{F16BP}|$ decreases, the calculated deviation indices rise, before levelling off for $|\epsilon^{PFK}_{F16BP}| < 0.01$. This value is likely to be around the upper end of the physiological region (approx. −0.01 to −0.0001), but there is no indication from Table 2 just where in this region ϵ^{PFK}_{F16BP} may lie. However, in this region, the value of ϵ^{PFK}_{F16BP} has virtually no effect on the distribution of the flux control coefficients (results not shown), so it is not particularly important to assign a value accurately. Therefore $\epsilon^{PFK}_{F16BP} = -0.005$ was chosen for the control analysis.

Concentration control coefficients

As well as flux control coefficients for a specified 'reference' flux, the matrix method [7] generates concentration control coefficients for all variable metabolites. Concentration control coefficients are very much the poor relatives to flux control coefficients, receiving little attention in the MCA literature. However, there are a number of specific uses of concentration control coefficients, exemplified by our calculation of the metabolite deviation indices D^S_{PFK} for indirect assignment of a value to ϵ^{PFK}_{F16BP}. We have also used them to calculate the effect on the patterns of metabolite distribution of the secondary changes in expression of the other glycolytic enzymes, as described in the preceding paper [1]. A further use is in quantifying the contribution of each variable metabolite to the flux control coefficient of an enzyme, E_i, as defined by Heinrich and Rapoport [18,19]:

$$C^J_i = 1 + \sum_S C^S_i \epsilon^i_S \quad (2)$$

where the summation is over all variable metabolites that are effectors of E_i. The first term shows that, in the absence of any other effect, increasing the activity of an enzyme will increase the flux by a proportional amount (i.e. $C^J_i = 1$). However, this proportional increase is modified by changes in concentrations of the effectors of E_i (the summation terms). For normal kinetics, each term in the summation will be negative: products and downstream feedback inhibitors have positive C^S_i, but negative ϵ^S_i, whereas the opposite holds for substrates and upstream feedforward activators. Thus the fact that enzymes have flux control coefficients less than one is a consequence of changes in the concentrations of their effectors. The value of each term in the summation quantifies the importance of the particular metabolite to the flux control coefficient. The implications for the flux control coefficient of PFK in the control analysis model we have used are described in the next section.

Table 4 Flux control coefficients for glycolytic enzymes of GUS control and PFK transgenic plants

C^J_E is the flux control coefficient of enzyme E over the glycolytic flux, and −0.000 signifies $-0.001 < C^J_E < 0.000$. Flux control coefficients were calculated using the computer program MetaCon.

Control coefficient	GUS-6	PFK-5	PFK-36	PFK-22
C^J_{PGM}	0.029	0.072	0.035	0.223
C^J_{PGI}	0.139	0.054	0.051	0.123
C^J_{PFK}	0.132	0.027	0.026	0.017
$C^J_{aldolase}$	−0.000	−0.000	−0.000	−0.000
C^J_{TPI}	−0.002	−0.000	−0.000	−0.000
$C^J_{GAPDH/PGK}$	0.001	0.000	0.000	0.000
C^J_{PGlyM}	−0.006	−0.000	0.000	0.000
$C^J_{enolase}$	0.005	0.000	0.000	0.000
C^J_{PK}	0.702	0.848	0.888	0.636

In addition to these specific uses, the general properties of concentration control coefficients are interesting. As a consequence of the existence of approximately equal numbers of positive and negative coefficients for most pathways, their values generally have much larger ranges of absolute values. This can be seen by comparing, for example, the last five rows of Table 3 with those in Table 4. The large values reflect the frequent occurrence of high physiological sensitivity of metabolite concentrations to enzyme activities, especially in sequences of near-equilibrium steps. This high sensitivity of metabolite concentrations to enzyme activities is a useful feature, but one that must be used with care. For example, it has enabled us to carry out a finite change analysis of the results of PFK overexpression [1], when flux changes revealed no information. In addition, we were able to assign an approximate value of ϵ^{PFK}_{F16BP} because of the relative sensitivities of concentration control coefficients to elasticities. However, this very sensitivity also means that the values of concentration control coefficients calculated using the matrix method are likely to be less reliable than corresponding flux control coefficients, and must be interpreted with circumspection if there is any doubt regarding the reliability of the data.

Flux control coefficients

The main purpose of this analysis was to determine the value of the flux control coefficient of each step over the pathway flux. These values are shown in Table 4. In those few cases where comparisons are possible, the model shows good agreement with experimental results. The crucial value is that of C^{J}_{PFK}, which is low, in all lines, entirely in agreement with the observation that overexpression of PFK had very little effect on either respiration or glycolysis in potato tuber [1,3,4]. Also the values calculated for the transgenic lines decline with increasing activity of PFK, exactly as would be expected for overexpression of an enzyme. The other important values in Table 4 are the high values for C^{J}_{PK} for all lines. In fact, although the last step of the model is defined as PK, it is merely a synonym for the metabolism of PEP, entailing its complete oxidation under aerobic conditions. Thus the significance of the last line of Table 4 is that the majority of flux control appears to reside in the fate of PEP (or in the breakdown of starch, which is not covered in this model), rather than in the glycolytic segment of metabolism. Irrespective of the control exerted by starch breakdown, the results in Table 4 predict that two to three times more control lies in the catabolism of PEP than in its production from G1P.

The negative flux control coefficients $C^{J}_{aldolase}$, C^{J}_{TPI} and C^{J}_{PGlyM}, as with the concentration control coefficients of incorrect sign, are a consequence of the negated elasticities described earlier. With the data to hand there is no way of assessing what their true values should be or what effect they would have on the other control coefficients. However, because the flux summation theorem is one of the equations used in calculating the control coefficients [13], if the negative coefficients were made positive (as presumably they are *in vivo*), it would be at the expense of the other flux control coefficients, one or more of which would have to be reduced to maintain their sum at 1. Without good estimates of the *in vivo* disequilibrium ratios, ρ, of the steps, no valid estimate of the corresponding control coefficients can be made. Unless the disequilibrium ratio is known to approach 1 it would be inaccurate to dismiss them as 'near-equilibrium', and thus with negligible control coefficients because, as we have mentioned in the preceding paper [1], simulation studies show that significant control can be invested in a series of steps that would previously have been defined as being near-equilibrium. In fact, whether these steps have small or large control coefficients belies the point of the argument. Enzymes such as PFK are targeted for genetic manipulation because they are believed to have large flux control coefficients. As both experiment and our model show, control lies elsewhere, at least in aged disks of potato tuber. Realizing this point is a first step to determining just where control really does lie. The inaccurate values of the elasticities, and hence of the control coefficients of aldolase, TPI, GAPDH, PGK and PGlyM, reflect the fact that study of these enzymes (and of pathway dynamics) has historically been subordinated to the study of postulated 'rate-limiting' enzymes. If the five steps in question do actually have significant control coefficients *in vivo*, they are as likely to be at the expense of PFK as of any other step, implying a further reduction in the true value of C^{J}_{PFK}.

Our model has indicated that the major portion of respiratory control in potato tuber lies outside the glycolytic sequence. What of the control of glycolysis itself? Removing the PK step from the model generates flux control coefficients in the GUS control tissue of PGM, PGI, PFK and enolase of 0.096, 0.46, 0.44 and 0.085 respectively. Again, these must be approximations because of the presence of the negative control coefficients. However, they still show reasonable agreement with the data of Burrell et al. [3], who observed that overexpression of PFK had no effect on anaerobic glycolysis. The stated value (0.44) of $C^{glycolysis}_{PFK}$ is actually an overestimate of the true *in vivo* value because terminating the pathway at PEP removes the elasticity ϵ^{PFK}_{PEP}, the existence of which serves to reduce $C^{glycolysis}_{PFK}$. In fact, it is the presence of strong feedback inhibition of PFK by PEP that is almost certainly the physiological reason for the low value of $C^{glycolysis}_{PK}$, as originally proved by Kacser and Burns [5] and described in the preceding paper [1]. In terms of our control analysis, the relative importance of the three effectors of PFK can be determined using eqn. (2):

$$C^{J}_{PFK} = 1 + C^{F6P}_{PFK}\epsilon^{PFK}_{F6P} + C^{F16BP}_{PFK}\epsilon^{PFK}_{F16BP} + C^{PEP}_{PFK}\epsilon^{PFK}_{PEP}.$$

Substituting values for ϵ^{PFK}_{S} from Table 1 and for C^{S}_{PFK} from Table 2:

$$C^{J}_{PFK} = 1 - 0.17 - 0.00 - 0.70 = 0.13$$

Thus the inhibition of PFK by PEP is quantitatively by far the most important of the factors we have considered in determining the low flux control coefficient of PFK. The stronger the effect of the feedback inhibition (i.e. the more negative is ϵ^{PFK}_{PEP}), the more flux control is removed from the inhibited step (PFK). This has been an important consideration in assigning the PFK kinetics as described in Appendix 2.

Confirmation that flux control is exerted downstream of PEP is obtained from the scaled metabolite changes in the PFK transgenic lines (Figure 2 of [1]). The large relative increases in F16BP concentration in the transgenic plants generate decreasing relative changes in PEP and pyruvate, ultimately leading to no increase in the rate of production of CO_2, or transfer of reducing equivalents to O_2. Thus assuming there are no significant changes in enzyme activities elsewhere (see [1] for further discussion), there is good corroboration that some control is exerted in the dephosphorylation of PEP, and in the oxidative metabolism of pyruvate.

Sensitivity analysis of the model

There is no doubt that a model such as this one, drawing as it does on a large number of experimental observations from a number of sources, and making a number of oversimplifications, is liable to be flawed. However, the successes, prediction of low flux control by PFK over both respiration and glycolysis, and reasonable agreement between observed and calculated deviation indices, are notable. This confirmation of the model's validity can be supported by a mathematical sensitivity analysis of the calculated control coefficients. It has been shown that control analysis models are much more sensitive to some variables (elasticities, etc.) than to others, and furthermore these sensitivities can be calculated from the variables themselves [14,15]. In particular, control coefficients are generally insensitive to changes in large substrate or product elasticities, although this is by no means an infallible rule. For this model a sensitivity analysis was carried out using the program MetaCon, to examine which elasticity values have the greatest effect on the results and hence the greatest potential to introduce error. Analysing the model for the GUS control line reveals that two elasticities, ϵ^{PFK}_{PEP} and ϵ^{PK}_{PEP}, have the largest effect on both C^{J}_{PFK} and C^{J}_{PK}, the two coefficients that are of most interest in this study. As the control coefficients are defined functions of the elasticities, the effect on the control coefficients of variation in the elasticities can be plotted (Figure 1). The two plots have a number of similarities. Variation of either elasticity from its calculated value ($\epsilon^{PFK}_{PEP} = -1.17, \epsilon^{PK}_{PEP} = 0.22$) leads to a change in C^{J}_{PK}, with compensating changes in C^{J}_{PGI}, C^{J}_{PFK} and C^{J}_{PGM}, but not in their

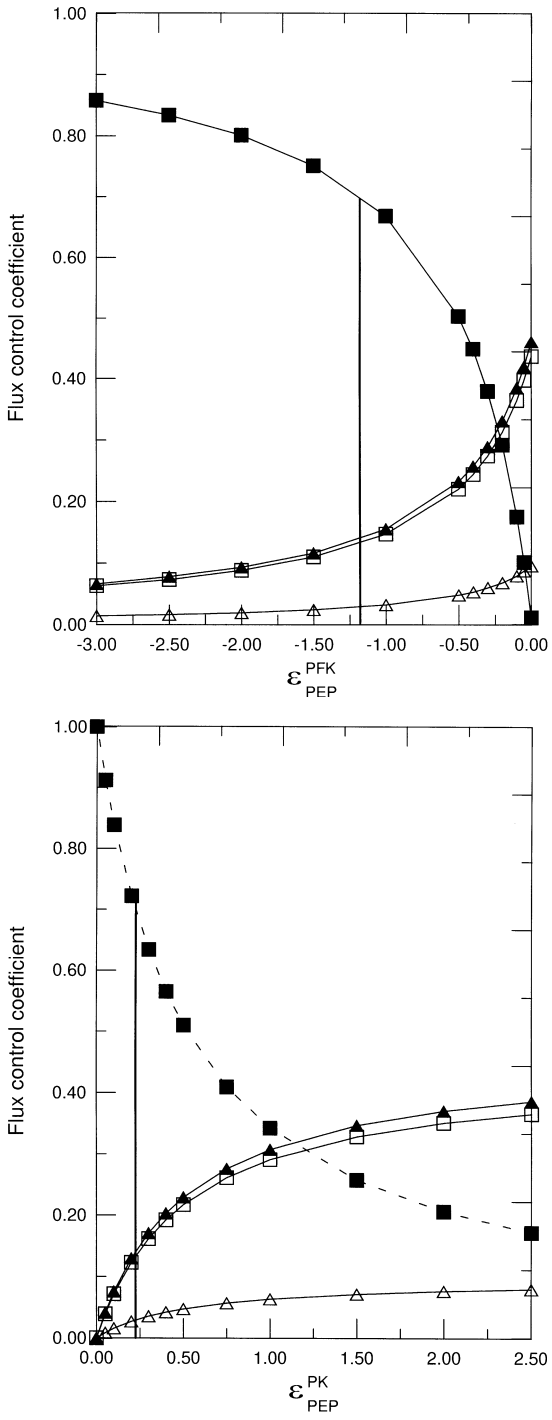

Figure 1 Variation of important flux control coefficients with critical elasticities

Control coefficients were calculated for different values of ϵ^{PK}_{PEP} or ϵ^{PFK}_{PEP} at fixed values of all other elasticities. The vertical line on each plot marks the *in vivo* estimate of the elasticity and the control coefficients calculated for that value. △, PGM; ▲, PGI; □, PFK; ■, PK. Control coefficients for other enzymes are not plotted because none of them increases above 0.05 for any of the values of the critical elasticities considered. Top, Variation with ϵ^{PFK}_{PEP}; bottom, variation with ϵ^{PK}_{PEP}.

relative values. Thus at all values of ϵ^{PFK}_{PEP} or ϵ^{PK}_{PEP} the order is $C^J_{PGI} > C^J_{PFK} > C^J_{PGM}$. The other control coefficients are virtually unaffected. Also, in both cases large changes away from the calculated values are required to significantly alter the distribution of control between the production and the consumption of PEP. Not unless ϵ^{PFK}_{PEP} is approximately 40 % (Figure 1, top), or ϵ^{PK}_{PEP} 250 % of its calculated value (Figure 1, bottom) does the control over the flux exerted by PEP consumption drop to less than 50 %. In fact, because we have used $n = 2$ rather than 4 in our calculation of PFK inhibition kinetics (see Appendix 2), our calculated ϵ^{PFK}_{PEP} is, if anything, likely to underestimate the true magnitude. In comparison, our value of ϵ^{PK}_{PEP} is likely to be an overestimate of the true value, as we have not taken product inhibition into account. As 'PK' represents catabolism of PEP, not just the single enzyme, the product inhibition, and hence our underestimate of the control actually exerted by PEP catabolism can be expected to be considerable. Therefore our estimates of the two most critical elasticities are likely to err on the side of overestimating the real control exerted by PFK over both glycolysis and respiration. Although the results of this sensitivity analysis are not conclusive proof of the correctness of the model, they provide further evidence to go with the experimental observations that the model does generate a good approximation to the flux control properties of the pathway.

There are two points worth mentioning with respect to the effect of ϵ^{PFK}_{PEP}. First, the calculated elasticity is quite large but it still has a major effect on the values of the control coefficients. Thus the general rule that large elasticities are relatively unimportant does not always hold. This rule was inferred for the effect of substrate and product elasticities of near-equilibrium enzymes, and care should be taken to restrict its application to this case. The rigorous calculation of sensitivities described here is more appropriate. Second, all the effects of varying the feedback inhibition of PEP on PFK cannot be simulated by varying ϵ^{PFK}_{PEP} as shown in Figure 1 (top). Because of the homoeostatic effect of PFK inhibition by PEP [1,20], the *in vivo* intermediate concentrations and hence their elasticities to aldolase, TPI, etc. are already influenced by PEP feedback of PFK, and these components are not affected by the variation of ϵ^{PFK}_{PEP} shown in Figure 1 (top), as they would be if the feedback strength of PEP on PFK were really altered and the pathway allowed to reach a new steady-state.

Conclusion

In this paper we have shown how the connectivity and summation theorems of MCA can be used to quantify the control properties of a pathway, and to successfully explain the consequences, for respiratory flux and glycolytic metabolites, of overexpressing active PFK in potato tubers. The approach is different from our previous one [1], and the data we used are largely complementary: although we used metabolite concentrations from the PFK transgenic lines, this was not necessary for the analysis of the control plants. Consequently, the method could be used to predict the likely outcome of genetic manipulation of enzymes on any particular tissue of interest. The only requirement would be the measurement of intermediate metabolite concentrations and a survey of kinetic data from the literature. However, as has been stated elsewhere [2,21] even if this approach were to identify step(s) with large flux control coefficient(s), massive degrees of overexpression will often lead to only modest increases in flux.

The success of the approach is pleasing, given the wide range of sources of the kinetic data used and the approximations made in setting up the model for analysis. Its success in explaining experimental data is further supported by its proven robustness to large changes in some crucial elasticities. However, the accuracy of our results will depend on the values of the control coefficients that could not be determined (those of aldolase, TPI,

GAPDH/PGK and PGM) and on the existence of interactions not included in our model. The potential problems with the type of analysis we have used have been discussed before. Some have been specifically mentioned in previous sections and it is unnecessary to enlarge further (for more detail see [8,11,14,15]). However, one specific problem we have largely ignored that must be addressed is the potential effect of fluxes through PFP and the pentose phosphate pathway. Whatever their effects on the glycolytic flux they have the ability to buffer metabolite changes, especially in G6P, F6P, F16BP, and GAP. They might explain the anomalous behaviour of these metabolites described in the preceding paper [1], and the poor agreement between the calculated and observed deviation indices for some metabolites. However, these effects are also overlooked by those who identify PFK as a likely target for overexpression to increase glycolytic flux. If PEP and the near-equilibrium reactions of the pentose phosphate pathway can have a homoeostatic effect on F16BP, GAP etc., then they must serve to attenuate the signal (increased F16BP) produced by PFK overexpression [22]. This point also reinforces the observations made in the preceding paper [1] regarding our limited knowledge of the behaviour of metabolic systems, which is still largely dominated by the concept of the rate-limiting step. Until more attention is paid to the behaviour and system properties of metabolic pathways, including the effects of 'near-equilibrium' steps, our understanding of metabolic control, let alone our ability to successfully manipulate major pathways as we wish, will remain poor.

The interactions that control metabolism in major biochemical pathways such as glycolysis are far too complex for us to yet grasp fully. However, whatever the nature of the important interactions – flux branching from or into other pathways, flux control exerted by, or regulatory effects exerted at, 'near-equilibrium' enzymes – the emphasis in approach must change to one based more on the study of systemic properties, rather than the current situation where the study of putative 'rate-limiting' steps is predominant. The model we have proposed is not a complete model of potato tuber glycolysis, and the use of MCA in the way we have described is but one approach to understanding biochemical systems. Additional techniques, such as computer simulation, would provide a complementary perspective, but require more data. Over the past two decades, theoretical approaches have revealed, and will continue to reveal, many empirical principles that have fundamentally altered our view of metabolic control. They have been somewhat less successful at interpreting the behaviour of specific metabolic pathways, but this is largely due to our ignorance of the real relationship between *in vitro* and *in vivo* phenomena. On the other hand, the answers that can be obtained from experiment are limited without a quantitative systemic approach by means of which to pose relevant questions. Despite the constraints and uncertainties, this study illustrates that existing biochemical knowledge can be sufficient to predict the outcome of experiments in genetic manipulation provided that an appropriate methodological approach such as MCA is used. Although in this case the MCA interpretation followed the experiments, we believe it is a model for an integrated approach combining theory, analysis, simulation and experiment. Only by adopting such an approach will rapid progress be made in understanding metabolic control.

S.T. is a Leverhulme Trust Special Research Fellow.

REFERENCES

1 Thomas, S., Mooney, P. J. F., Burrell, M. M. and Fell, D. A. (1997) Biochem. J. **322**, 111–117
2 Small, J. R. and Kacser, H. (1993) Eur. J. Biochem. **213**, 613–624
3 Burrell, M. M., Mooney, P. J. F., Blundy, M., Carter, D., Wilson, F., Green, J., Blundy, K. S. and ap Rees, T. (1994) Planta **194**, 95–101
4 Mooney, P. J. F. (1994) Ph.D. Thesis, University of London
5 Kacser, H. and Burns, J. A. (1973) Symp. Soc. Exp. Biol. **27**, 65–104
6 Kacser, H., Burns, J. A. and Fell, D. A. (1995) Biochem. Soc. Trans. **23**, 341–366
7 Fell, D. A. and Sauro, H. M. (1985) Eur. J. Biochem. **148**, 555–561
8 Groen, A. K., van Roermund, C. W. T., Vervoorn, R. C. and Tager, J. M. (1986) Biochem. J. **237**, 379–389
9 Fell, D. A. and Snell, K. (1988) Biochem. J. **256**, 96–101
10 Kashiwaya, Y., Sato, K., Tsuchiya, N., Thomas, S., Fell, D. A., Veech, R. L. and Passonneau, J. V. (1994) J. Biol. Chem. **269**, 25502–25514
11 Fell, D. A. (1992) Biochem. J. **286**, 313–330
12 Stitt, M. (1989) Plant Physiol. **89**, 628–633
13 Thomas, S. and Fell, D. A. (1993) Biochem. J. **292**, 351–360
14 Small, J. R. and Fell, D. A. (1990) Eur. J. Biochem. **191**, 413–420
15 Thomas, S. and Fell, D. A. (1994) J. Theor. Biol. **167**, 175–200
16 Sasaki, T., Tadokoro, K. and Suzuki, S. (1973) Phytochemistry **12**, 2843–2849
17 Small, J. R. and Kacser, H. (1993) Eur. J. Biochem. **213**, 625–640
18 Heinrich, R. and Rapoport, T. (1975) BioSystems **7**, 130–136
19 Heinrich, R., Rapoport, S. M. and Rapoport, T. A. (1977) Prog. Biophys. Mol. Biol. **32**, 1–82
20 Hofmeyr, J.-H. S. and Cornish-Bowden, A. (1991) Eur. J. Biochem. **200**, 223–236
21 Fell, D. A. and Thomas, S. (1995) Biochem. J. **311**, 35–39
22 Thomas, S. and Fell, D. A. (1996) J. Theor. Biol. **182**, 285–298

APPENDIX 1

Model details used in control analysis

Enzyme kinetic parameters

Enzyme kinetic parameters for the glycolytic enzymes in potato tuber are scarce. Therefore we have used published parameters from plants and closely related tissues wherever possible. The kinetics and elasticities of *S. tuberosum* PFK are detailed in Appendix 2. Full details of the kinetics of the other steps are included in Table A1 and in its footnotes. Note that the kinetic parameters used for aldolase and TPI are irrelevant because the disequilibrium ratios are always greater than 1. However, they are included here for completeness, and to give an indication of the information that is available for carrying out control analyses of this kind.

Equations for elasticities

(1) One-substrate one-product enzymes (PGM, PGI, TPI, PGlyM and enolase). Generic terms have been used (S = substrate, P = product) in the following equations:
(a) Near-equilibrium approximation [1]:

$$\epsilon_s = 1/(1-\rho)$$

$$\epsilon_p = -\rho/1-\rho)$$

where disequilibrium ratio, $\rho = (P/S)/K_{eq}$.
(b) Full kinetic expression

$$\epsilon_s = \frac{1}{1-\rho} - \frac{S/K_s}{1+S/K_s+P/K_P}$$

$$\epsilon_P = \frac{-\rho}{1-\rho} - \frac{P/K_P}{1+S/K_s+P/K_P}$$

Table A1 Mechanisms and kinetic parameters of enzymes used in the model

Step	Mechanism	Parameters
PGM	Reversible one-substrate one-product Michaelis–Menten	Near-equilibrium assumption $K_{eq} = 17.2$[a]
PGI	Reversible one-substrate one-product Michaelis–Menten	$K_{G6P} = 0.27$ mM[b] $K_{F6P} = 0.15$ mM[c] $K_{eq} = 0.298$[a]
PFK	see Appendix 2	
Aldolase	Ordered uni–bi mechanism; GAP is first product released[d]	$K_{F16BP} = 1.75\ \mu$M[e] $K_{GAP} = 1.5$ mM[f] $K_{DHAP} = 1.5$ mM[f] $K_{eq} = 0.081$ mM[a]
TPI	Reversible one-substrate one-product Michaelis–Menten	$K_{GAP} = 0.33$ mM[g] $K_{DHAP} = 0.64$ mM[h] $K_{eq} = 0.0455$ mM[a]
GAPDH/PGK		Near-equilibrium assumption $K_{eq} = 1.724$[a]
PGlyM	Reversible one-substrate one-product Michaelis–Menten	$K_{3PGA} = 0.330$ mM[i] $K_{2PGA} = 0.06$ mM[i] $K_{eq} = 0.2$[a]
Enolase	Reversible one-substrate one-product Michaelis–Menten	$K_{2PGA} = 0.15$ mM[j] $K_{PEP} = 0.15$ mM[j] $K_{eq} = 6.3$[a]
PK	Partial rapid equilibrium Bi Bi[k]	$K_{PEP} = 0.02$ mM $K_{ADP} = 0.02$ mM $K_{ATP} = 0.086$ mM $K_{Pyr} = 1$ mM $K_{eq} = 6451.6$[a]

[a]From [2].

[b]Pea enzyme [3]. However, most values in [4] are of the order of 0.1 mM.

[c]Approximated by comparison of magnitudes of K_{G6P} and K_{F6P} in [4].

[d]From [5].

[e]Mean of values for the enzymes from spinach, wheat and corn leaves, and pea shoot (all cytoplasmic enzymes) from [5].

[f]Approximate value from yeast and rabbit liver [2] and rabbit muscle [6]. However, values for rabbit liver from [6] are of the order of 10^{-4} M.

[g]Mean of values for: pea seed [7], pea leaf chloroplast and cytoplasm [8]. Also consistent with the values in [4] for mammalian enzymes (0.32–0.5 mM) but not yeast (1.27 mM).

[h]Approximated by comparison of magnitudes of K_{GAP} and K_{DHAP} in [4].

[i]Cytosolic enzyme in castor plant (*Ricinus communis*) [9].

[j]K_{2PGA} is well documented. However, the value of 0.83 mM for the potato tuber enzyme quoted in [10] is very different from those reviewed by Wold [11], including plant tissues such as peas and soya bean (0.1–0.25 mM), and that of Sinha and Brewer [12] for a spinach leaf enzyme (55 μM). Therefore 0.15 mM was used for K_{2PGA} and 0.15 mM for K_{PEP}.

[k]Ireland et al. [13] have determined that the reaction catalysed by the cytosolic enzyme of the castor plant (*R. communis*) is ordered, with PEP binding before ADP, and pyruvate being released before ATP. To simplify the kinetics, the enzyme is modelled as a Partial Rapid Equilibrium Bi Bi System (see [14], p. 591 onwards). K_{PEP} and K_{ATP} are calculated from the data provided by Ireland et al. [13]. No product (ADP, PK) binding values are provided by Ireland et al. [13]; we have compared their values with values for rabbit muscle from [2]. The values from [13] are approx. one-tenth those for rabbit muscle, consequently the values given in [2] for K_{ATP} and K_{Pyr} were divided by 10, to give the values used.

(2) GAPDH/PGK. Near-equilibrium approximation is used, except that:

$$\rho = [3PGA] \times [NADH] \times [ATP]/([G3P] \times [P_i] \times [NAD] \times [ADP])/\{K_{eq}(GAPDH) \times K_{eq}(PGK)\}.$$

(3) Aldolase.

$$\epsilon^{aldolase}_{F16BP} = \frac{1}{1-\rho} - \frac{[F16BP]/K_{F16BP}}{1+\frac{[F16BP]}{K_{F16BP}}+\frac{[GAP][DHAP]}{K_{GAP}K_{DHAP}}+\frac{[DHAP]}{K_{DHAP}}}$$

$$\epsilon^{aldolase}_{GAP} = \frac{-\rho}{1-\rho} - \frac{\frac{[GAP][DHAP]}{K_{GAP}K_{DHAP}}}{1+\frac{[F16BP]}{K_{F16BP}}+\frac{[GAP][DHAP]}{K_{GAP}K_{DHAP}}+\frac{[DHAP]}{K_{DHAP}}}$$

$$\epsilon^{aldolase}_{DHAP} = \frac{-\rho}{1-\rho} - \frac{\frac{[GAP][DHAP]}{K_{GAP}K_{DHAP}}+\frac{[DHAP]}{K_{DHAP}}}{1+\frac{[F16BP]}{K_{F16BP}}+\frac{[GAP][DHAP]}{K_{GAP}K_{DHAP}}+\frac{[DHAP]}{K_{DHAP}}}$$

where $\rho = ([DHAP] \times [GAP])/F16BP/K_{eq}$.

(4) Pyruvate kinase.

$$\epsilon^{PK}_{PEP} = \frac{1}{1-\rho} - \frac{\frac{[PEP]}{K_{PEP}}+\frac{[PEP][ADP]}{K_{PEP}K_{ADP}}}{1+\frac{[PEP]}{K_{PEP}}+\frac{[PEP][ADP]}{K_{PEP}K_{ADP}}+\frac{[Pyr][ATP]}{K_{Pyr}K_{ATP}}+\frac{[ATP]}{K_{ATP}}}$$

References

1 Groen, A. K., van Roermund, C. W. T., Vervoorn, R. C. and Tager, J. M. (1986) Biochem. J. **237**, 379–389
2 Barman, T. E. (1969) Enzyme Handbook, Springer-Verlag, Berlin
3 Takeda, Y., Hizukuri, S. and Nikuni, Z. (1967) Biochim. Biophys. Acta **146**, 568–575
4 Noltmann, E. A. (1972) Enzymes 3rd Ed. **6**, 272–354
5 Horecker, B. L., Tsolas, O. and Lai, C. Y. (1972) Enzymes 3rd Ed. **7**, 213–280
6 Morse, D. E. and Horecker, B. L. (1968) Adv. Enzymol. Relat. Areas Mol. Biol. **31**, 125–181
7 Turner, D. H., Blanch, E. S., Gibbs, M. and Turner, J. F. (1965) Plant Physiol. **40**, 1146–1150
8 Anderson, L. E. (1971) Biochim. Biophys. Acta **235**, 237–244
9 Botha, F. C. and Dennis, D. T. (1986) Arch. Biochem. Biophys. **245**, 96–103
10 Boser, H. (1959) Z. Physiol. Chem. **315**, 163–170
11 Wold, F. (1971) Enzymes 3rd Ed. **5**, 499–538
12 Sinha, S. and Brewer, J. M. (1984) Plant Physiol. **74**, 834–840
13 Ireland, R. J., De Luca, V. and Dennis, D. T. (1980) Plant. Physiol. **65**, 1188–1193
14 Segel, I. H. (1975) Enzyme Kinetics, John Wiley, New York

APPENDIX 2

Kinetic details of PFK used in control analysis

The most complete set of kinetic data for potato tuber was collected by Sasaki et al. [1]. They determined that $K_{F6P} = 0.21$ mM and measured the inhibition of the enzyme by PEP, which changes the activity curve from hyperbolic in the absence of PEP to sigmoidal in its presence, the sigmoidicity increasing with increasing PEP. They also studied the action of other inhibitors, but PEP had by far the strongest effect. However, they did not study product inhibition by F16BP, nor did they calculate parameters for PEP inhibition. As there were no data in their paper for product inhibition we could not calculate ϵ^{PFK}_{F16BP}. Therefore we had to try to estimate this value from the behaviour of the model's concentration control coefficients as described in the main text. However, we could calculate kinetic parameters for the PEP inhibition data from Figure 5 in [1]. We modelled PFK as a Monod–Wyman–Changeux concerted enzyme [2], with exclusive binding of PEP to the T state:

$$v = \frac{\frac{V_m[F6P]}{K_{F6P}}\left(1+\frac{[F6P]}{K_{F6P}}\right)^{n-1}}{\left(1+\frac{[F6P]}{K_{F6P}}\right)^{n} + L\left(1+\frac{[PEP]}{K_{PEP}}\right)^{n}} \quad \text{(A1)}$$

Parameter estimation was attempted by the following means.

1. Linear transformation (see [3]). This generated impossible parameters (e.g. $K_{\mathrm{F6P}} = -16.7$), and was discounted.
2. Unweighted non-linear least-squares regression. The best fit to the published data required different parameters over low and high PEP ranges. The best fit over the range of cytosolic PEP found in the different tuber lines (0.07 to 0.45 mM) was given by $K_{\mathrm{F6P}} = 0.29$ mM (not 0.21 mM, the value calculated by [1] in the absence of PEP), $L = 1, n = 2, K_{\mathrm{PEP}} = 0.018$ mM, with 96.6 % of variance explained.

Inspection of the plot for these parameters showed poor agreement at higher F6P concentrations, because the model fitted is for inhibition in a K system, whereas the data from [1] indicate an effect on V as well. However, fitting an inhibition to a V system will not generate sigmoidal kinetics with respect to F6P in the presence of PEP [3], as had been observed by Sasaki et al. [1]. A compromise was achieved by fitting concentrations up to only 2 mM. This encompasses the range observed in the potato tubers, while limiting the analysis to the region where the fitted model shows greatest agreement with the experimental data.

Received 4 July 1996/1 October 1996; accepted 14 October 1996

For the Monod–Wyman–Changeux equation (A1) the elasticities are:

$$\epsilon^{\mathrm{PFK}}_{\mathrm{F6P}} = \frac{1+\dfrac{n[\mathrm{F6P}]}{K_{\mathrm{F6P}}}}{1+\dfrac{[\mathrm{F6P}]}{K_{\mathrm{F6P}}}} - \frac{\dfrac{n[\mathrm{F6P}]}{K_{\mathrm{F6P}}}}{L\dfrac{\left(1+\dfrac{[\mathrm{PEP}]}{K_{\mathrm{PEP}}}\right)^{n}}{\left(1+\dfrac{[\mathrm{F6P}]}{F_{\mathrm{F6P}}}\right)^{n-1}} + \left(1+\dfrac{[\mathrm{F6P}]}{K_{\mathrm{F6P}}}\right)}$$

$$\epsilon^{\mathrm{PFK}}_{\mathrm{PEP}} = \frac{-\dfrac{nL[\mathrm{PEP}]}{K_{\mathrm{PEP}}}}{L\left(1+\dfrac{[\mathrm{PEP}]}{K_{\mathrm{PEP}}}\right) + \dfrac{\left(1+\dfrac{[\mathrm{F6P}]}{K_{\mathrm{F6P}}}\right)^{n}}{\left(1+\dfrac{[\mathrm{PEP}]}{K_{\mathrm{PEP}}}\right)^{n-1}}}$$

References

1 Sasaki, T., Tadokoro, K. and Suzuki, S. (1973) Phytochemistry **12**, 2843–2849
2 Monod, J., Wyman, J. and Changeux, J.-P. (1965) J. Mol. Biol. **12**, 88–118
3 Segel, I. H. (1975) Enzyme Kinetics, John Wiley, New York